Available online at www.sciencedirect.com
ScienceDirect
Estuarine, Coastal and Shelf Science 72 (2007) 16–32
ESTUARINE COASTAL AND SHELF SCIENCE
www.elsevier.com/locate/ecss

Remote sensing reflectance and inherent optical properties in the mid Chesapeake Bay

Maria Tzortziou [a,c,*], Ajit Subramaniam [b], Jay R. Herman [c], Charles L. Gallegos [d], Patrick J. Neale [d], Lawrence W. Harding Jr. [e]

[a] University of Maryland, Earth System Science Interdisciplinary Center, College Park, MD 20742, USA
[b] Lamont Doherty Earth Observatory, Columbia University, Palisades, NY 10964, USA
[c] NASA/Goddard Space Flight Center, Greenbelt, MD 20771, USA
[d] Smithsonian Environmental Research Center, Edgewater, MD 21037, USA
[e] University of Maryland Center for Environmental Science, Horn Point Laboratory, Cambridge, MD 21613, USA

Received 14 September 2005; accepted 21 September 2006
Available online 13 November 2006

Abstract

We used an extensive set of bio-optical data to examine the relationships between inherent optical properties and remotely sensed quantities in an optically complex and biologically productive region of the Chesapeake Bay. Field observations showed that the chlorophyll algorithms used by the MODIS (MODerate resolution Imaging Spectroradiometer) ocean color sensor (i.e. Chlor_a, chlor_MODIS, chlor_a_3 products) do not perform accurately in these Case 2 waters. This is because, at high concentrations of chlorophyll, all MODIS algorithms are based on empirical relationships between chlorophyll concentration and blue:green wavelength remote sensing reflectance (R_{rs}) ratios that do not account for the typically strong blue-wavelength absorption by non-covarying, dissolved and non-algal particulate components. We found stronger correlation between chlorophyll concentration and red:green R_{rs} ratios (i.e. $R_{rs}(677)/R_{rs}(554)$). Regionally-specific algorithms that are based on the phytoplankton optical properties in the red wavelength region provide a better basis for satellite monitoring of phytoplankton blooms in these Case 2 waters. Our estimates of f/Q (proportionality factor in the relationship between R_{rs} and the ratio of water backscattering, b_b, and absorption, a, coefficients, $b_b/(a + b_b)$) were not considerably different from f/Q previously estimated for same measurement geometry but Case 1 waters. Variation in surface b_b significantly affected R_{rs} magnitude across the visible spectrum and was most strongly correlated ($R^2 = 0.88$) with observed variability in R_{rs} at 670 nm. Surface values of particulate backscattering were strongly correlated with non-algal particulate absorption, a_{nap} ($R^2 = 0.83$). These results, along with the measured backscattering fraction and non-algal particulate absorption spectral slope, indicate that suspended non-algal particles with high inorganic content are the major water constituents regulating b_b variability in the studied region of the Chesapeake Bay. Remote retrieval of surface a_{nap} from $R_{rs}(670)$ could be used in conjunction with inversion of UV-blue wavelengths to separate contribution by non-algal particles and colored dissolved organic matter to total light absorption, and monitor non-algal suspended particle concentration and distribution in these Case 2 waters.

Keywords: bio-optics; satellite retrievals; Case 2; estuaries; coastal waters

1. Introduction

Changes in the concentrations and distribution of organic and inorganic, particulate and dissolved substances are of major water quality and ecological concern in the Chesapeake Bay estuary. Increased nutrient loadings in recent years, driven mainly by human population growth and changes in land use, have increased phytoplankton concentrations above historical levels (Harding and Perry, 1997). Changes in particulate and dissolved substances are linked to important processes in the estuary, such as freshwater river discharges, nutrient and light availability, tidal mixing, bottom resuspension, and microbial

* Corresponding author. NASA/Goddard Space Flight Center, Code 613.3, Bldg 33, Greenbelt, MD 20771, USA.
E-mail address: martz@code613-3.gsfc.nasa.gov (M. Tzortziou).

0272-7714/$ - see front matter © 2006 Elsevier Ltd. All rights reserved.
doi:10.1016/j.ecss.2006.09.018

activity (e.g. Kemp and Boynton, 1992; Malone, 1992). Because the composition and concentrations of in-water constituents influence optical characteristics, in-situ measurements of optical properties have been made by several ship-based monitoring programs during the last decades to examine water quality and assess progress in reversing eutrophication in the Bay (e.g. Glibert et al., 1995; Johnson et al., 2001). By using appropriate bio-optical algorithms, remote sensing of "ocean color" offers the capability of extending field observations beyond the restricted in-situ sampling domain. Several aircraft ocean-color instruments (using both "passive" and "active" systems) have been used to remotely measure surface chlorophyll-a concentrations [chl-a] and determine changes in phytoplankton biomass in the Chesapeake Bay (e.g. Hoge and Swift, 1981; Harding et al., 1992; Lobitz et al., 1998). However, only a limited number of studies have been published on the interpretation of satellite ocean color imagery and the applicability of currently used satellite algorithms for these optically complex estuarine waters (e.g. Harding et al., 2005).

In order to use satellite ocean color to extract information on water composition, it is necessary to develop effective bio-optical algorithms relating the remotely sensed water reflectance either directly to surface concentrations of optically significant water constituents (empirical algorithms; e.g. Clark, 1997; O'Reilly et al., 2000), or to their optical properties based on principles derived from radiative transfer theory (semi-analytical inversion models; e.g. Garver and Siegel, 1997; Maritorena et al., 2002). Since the launch of the Coastal Zone Color Scanner (CZCS) in October 1978, satellite ocean color has contributed significantly to gaining a better understanding of biological activity in open-ocean "Case 1" waters where phytoplankton and co-varying material are the major optical components (e.g. Yentsch, 1993; Longhurst et al., 1995; Gregg and Conkright, 2001). With more channels in the visible part of the spectrum, CZCS's follow-on sensor SeaWiFS (Sea-viewing Wide Field of view Sensor; launched in 1997) and the newer instrument MODIS (MODerate resolution Imaging Spectroradiometer, launched in 1999) allowed for further improvements in satellite retrievals of biogeochemical variables in Case 1 waters (e.g. Yoder and Kennelly, 2003; Carder et al., 2004; McClain et al., 2004). A more difficult challenge, however, has been developing bio-optical algorithms suitable for use in optically complex "Case 2" waters, like the Chesapeake Bay, where multiple, co-existing but not necessarily co-varying, dissolved and particulate, marine and terrigenous substances affect ocean color (e.g. Morel and Prieur, 1977; Carder et al., 1991; Ruddick et al., 2001; Binding et al., 2003; Boss et al., 2004; Darecki and Stramski, 2004; Magnuson et al., 2004; Dall'Olmo et al., 2005).

Harding et al. (2005) used SeaWiFS [chl-a] data and in-situ measurements of water reflectance and [chl-a] to examine the accuracy of satellite observations and the applicability of the SeaWiFS empirical chlorophyll algorithm OC4v4 (O'Reilly et al., 2000) for the Chesapeake Bay and Middle Atlantic Bight. They found that SeaWiFS reliably captured seasonal and inter-annual variability of phytoplankton biomass in the lower Bay. However, the OC4v4 algorithm significantly overestimated chlorophyll in the upper-mesohaline and oligohaline Chesapeake Bay due to strong absorption by dissolved organic matter and non-algal particles that are not sufficiently accounted for in this empirical chlorophyll algorithm (Harding et al., 2005).

These studies underscore the need to develop more accurate algorithms for Case 2 waters based on detailed in-situ bio-optical characteristics. However, certain optical properties of the Chesapeake Bay remain poorly characterized. Magnuson et al. (2004) used an extensive set of bio-optical data to parameterize and validate the semi-analytical Garver-Siegel-Maritorena (GSM01) model (Maritorena et al., 2002) for the Chesapeake Bay and the Mid-Atlantic Bight. Their efforts were limited by the scarcity of data on backscattering (b_b) in Chesapeake Bay. Due to the lack of in-situ data, modeling of b_b is often based on assumptions regarding scattering angular shape, backscattering magnitude, and spectral dependence. According to Magnuson et al. (2004) the lack of b_b measurements in the Bay affected their backscattering parameterizations and limited their ability to evaluate the GSM01 model's backscattering product. Tzortziou et al. (2006) recently applied detailed in-situ data and radiative transfer model calculations to examine b_b variability and modeling of backscattering processes for the mid Chesapeake Bay. They found that b_b was well characterized by a Fourier-Forand phase function, and that the average backscattering fraction was lower than the commonly assumed value of 0.018. However, information remains scarce on the contribution of various water constituents to the backscattering characteristics of Chesapeake Bay, and this lack of information has hindered the application of remotely sensed ocean color data to the remote retrieval of particulate backscattering variability in these Case 2 waters.

Previous studies have shown that the remote sensing reflectance R_{rs}, defined as the upwelling radiance emerging from the ocean divided by the downwelling irradiance reaching the water surface, is, to a first approximation, proportional to the ratio of backscattering, b_b, and absorption, a, coefficients, $b_b/(a + b_b)$ (e.g. Morel and Prieur, 1977). However, the magnitude and geometrical structure (or shape) of the upwelling radiance field within the ocean depend on both the inherent optical properties of the water (IOPs; e.g. volume scattering function (VSF) and a), as well as other factors (e.g. solar zenith angle, aerosol load) that affect illumination conditions (Austin, 1974; Morel and Gentili, 1991, 1993). Measurements and theoretical studies of the effects of these parameters on the relationship between R_{rs} and the ratio $b_b/(a + b_b)$ have been performed for Case 1 waters (e.g. Voss, 1989; Morel and Mueller, 2002; Voss and Morel, 2005). Further studies are needed for Case 2 waters, like the Chesapeake Bay.

In this paper, we present detailed in-situ bio-optical measurements from a region of the mid Chesapeake Bay, including new data on particulate backscattering, and examine relationships between remote sensing reflectance spectra and IOPs for improved remote retrievals of biogeochemical variables in

these Case 2 waters. Our main objectives were to: (i) assess the applicability of the chlorophyll algorithms currently used by SeaWiFS' successor MODIS, and examine alternative chlorophyll algorithms based on the red wavelengths where absorption by non-algal particles and dissolved matter are minimal; (ii) evaluate variability in the relationship between R_{rs} and $b_b/(a+b_b)$ for our measurement geometry and compare our results for these Case 2 waters with previous studies for Case 1 waters; (iii) determine the relative roles of algal and non-algal particles in backscattering and examine methods for remote retrieval of surface b_b and suspended particulate matter in these waters.

2. Theoretical background

Remote sensing of ocean color relies on detecting the light signal that leaves the water surface and reaches a sensor onboard a satellite, carrying with it information on IOPs of the water. Ocean remote sensing reflectance, R_{rs}, is related to backscattering, which redirects downwelling photons to travel upward and eventually leave the water surface, and absorption, which converts photons to heat or chemical energy. As upward traveling photons exit the water they interact with the air–water interface by refraction and internal reflection. R_{rs} can, therefore, be related to backscattering and absorption according to (e.g. Austin, 1974; Preisendorfer, 1976; Gordon et al., 1975; 1988; Lee et al., 1994):

$$R_{rs}(\lambda) = \frac{f(\lambda)}{Q(\lambda)} \cdot \frac{t_{(w,a)} t_{(a,w)}}{n_w^2} \cdot \frac{b_b(\lambda)}{a(\lambda)+b_b(\lambda)} \quad (1)$$

where $b_b(\lambda)$ is the total backscattering coefficient at wavelength λ, $a(\lambda)$ is the total absorption coefficient, $t_{(w,a)}$ is the water–air transmittance, $t_{(a,w)}$ is the transmittance from air to water, and n_w is the real part of the refractive index of the water. The quantity f is a complex function of wavelength, water IOPs (single scattering albedo and volume scattering function), solar zenith angle (θ_o), aerosol optical thickness, and surface roughness (Gordon et al., 1975; Kirk, 1984; Morel and Mueller, 2002). The quantity Q is the ratio of upwelling irradiance to upwelling radiance, $Q(\lambda) = E_u(\lambda)/L_u(\lambda)$ (Austin, 1974). Therefore, Q is influenced by the processes and environmental variables that affect the geometrical structure of the anisotropic upward radiance field (i.e. IOPs and environmental variables mentioned above, direction of upward traveling photons, and azimuth angle) (Morel and Mueller, 2002).

Variability in the ratio f/Q and its implications in ocean color remote sensing have been the focus of several theoretical studies. Early studies showed that the quantity f (dimensionless) has an average value of about 0.32–0.33 (Gordon et al., 1975; Morel and Prieur, 1977) when the sun is near zenith. However, according to Morel and Mueller (2002) the global range of variation in f is from about 0.3 to 0.6. Morel and Gentili (1993) found that Q values generally range from 3 to 6 sr. According to their study, both the f and Q functions increase with solar zenith angle. Therefore, the f/Q ratio would be expected to be less dependent on solar zenith angle than either f or Q alone. Their study showed that f/Q is relatively independent of θ_o for sun and viewing angles expected for the MODIS orbit, with average $f/Q = 0.0936$, 0.0944, 0.0929, and 0.0881 (SD = 0.005), for $\lambda = 440$, 500, 565, and 665 nm, respectively. Gordon et al. (1988) estimated that $f/Q = 0.0949$, for $\theta_o \geq 20°$. Thus, in various bio-optical algorithms that relate R_{rs} to IOPs, f/Q is assumed to be independent of wavelength and solar zenith angle (e.g. the MODIS semi-analytical chlorophyll algorithm; Carder et al., 2002).

Using detailed radiative transfer computations, Morel and Mueller (2002) showed that f/Q varies within the range 0.08–0.15 sr^{-1}. For simplicity, Morel and Mueller performed their calculations for homogeneous Case 1 waters, which allowed them to model all water IOPs (a, b_b, and VSF) as a function of the chlorophyll-a concentration (Morel et al., 2002). Their theoretical computations of Q showed very good agreement with measurements of radiance distribution performed by Voss and Morel (2005) over a large range of chlorophyll concentrations in the Case 1 waters of Baja California. The degree of agreement between theoretical computations and measurements of f/Q variability in Case 2 waters, however, remains unknown. One of the main objectives of this paper is to examine variability in the quantity f/Q and, as a result, in the relationship of R_{rs}: $b_b/(a+b_b)$, for the geometry of our measurements and over a wide range of bio-optical and environmental conditions for the Case 2 Chesapeake Bay waters.

3. Methods

3.1. Location and duration of measurements

Measurements were performed at four stations in the Chesapeake Bay designated: Poplar Island (PI), Herring Bay (HB), Tilghman Island (TI) and Jetta (JT) (38.71–38.89° N latitude, 76.34–76.54° W longitude). These stations were located in the upper mesohaline region of the Bay and included sites in both lateral and mid-channel waters (Fig. 1). Data were collected during 17 cruises performed between June–November 2001 and May–November 2002. All stations were sampled during each cruise, except from station JT on 6 June 2002 and stations HB and PI on 8 November 2002. Measurements performed in rough waters or under highly variable atmospheric conditions were not included in our analysis.

3.2. In-situ and laboratory measurements of water optical characteristics

Vertical profiles of total (minus pure water) attenuation, $c_{t-w}(\lambda,z)$, and absorption, $a_{t-w}(\lambda,z)$, were measured using a WETLabs AC-9 (Table 1). The AC-9 was calibrated annually by the manufacturer. Clear water calibrations were not carried out, but air tracking was done with every cleaning, before and after every cruise. Instrument drift is only a very small (and negligible) fraction of measured coefficients in such optically thick waters as the upper and mid portion of the Chesapeake Bay. Measurements were corrected for the

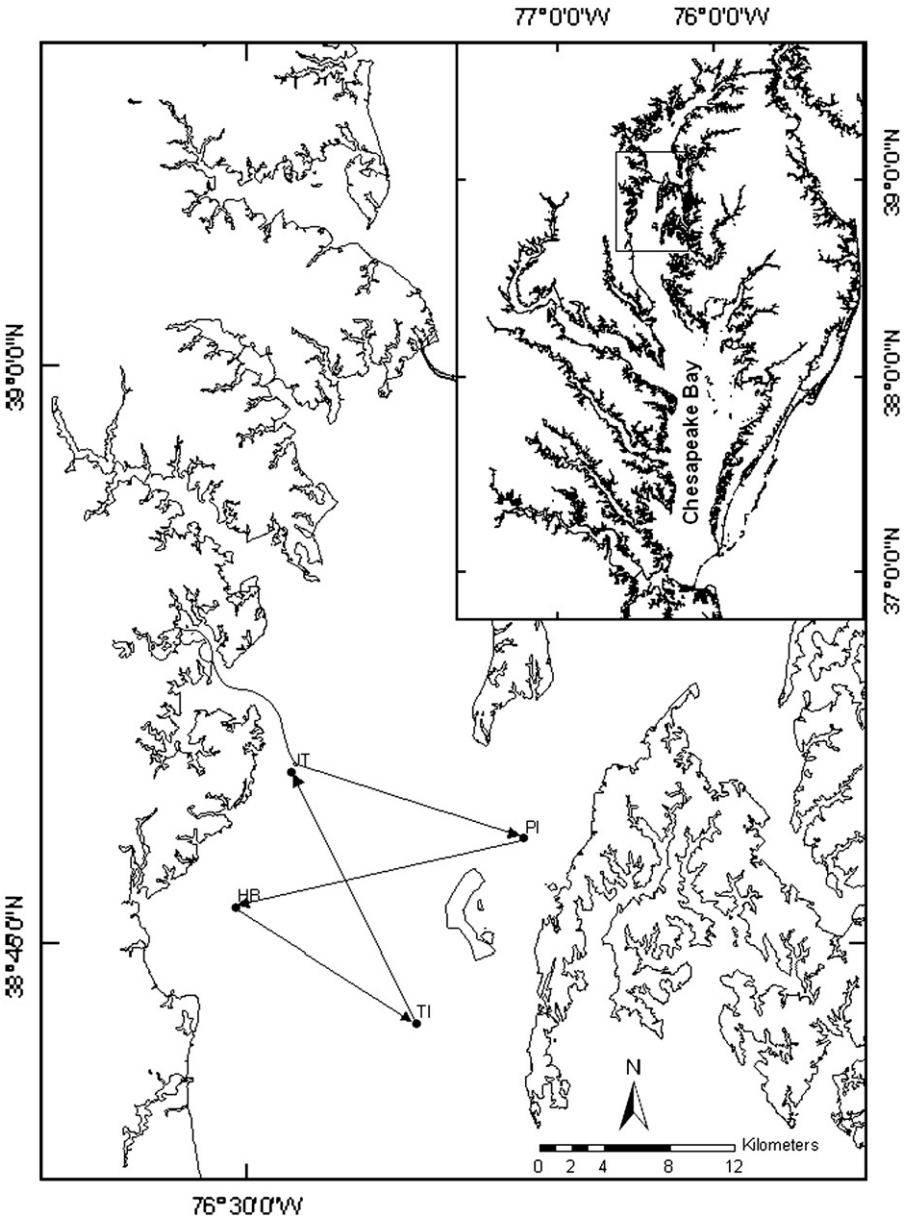

Fig. 1. Location of in-situ measurements (stations HB, PI, TI and JT) and cruise track. The starting point during our cruises was the SERC dock located in the Rhode River sub-estuary, along the western shore of the Chesapeake Bay.

Table 1
Measurements of IOPs and radiation fields

Measured quantities	Wavelengths (in nm)	Instrument used
Total absorption (minus absorption by pure water), a_{t-w}	412, 440, 488, 510, 532, 554, 650, 676, 715	AC-9
Total attenuation (minus attenuation by pure water), c_{t-w}	412, 440, 488, 510, 532, 554, 650, 676, 715	AC-9
Total backscattering, b_b	450, 530, 650	ECOVSF3
Phytoplankton absorption, a_{phyt}	290–750 (1 nm resolution)	CARY-IV
Non-algal particulate absorption, a_{nap}	290–750 (1 nm resolution)	CARY-IV
CDOM absorption, a_{CDOM}	290–750 (1 nm resolution)	CARY-IV
In-water upwelling radiance profiles, L_u	400, 412, 443, 455, 490, 510, 532, 554, 564, 590, 625, 670, 684, 700	Satlantic, MicroPro
In-water downwelling irradiance profiles, E_d	400, 412, 443, 455, 490, 510, 532, 554, 564, 590, 625, 670, 684, 700	Satlantic, MicroPro
In-water upwelling irradiance profiles, E_u	412, 443, 490, 510, 554, 665, 684	Satlantic, OCI-200
In-water downwelling irradiance profiles, E_d	325, 340, 380, 412, 443, 490, 510, 532, 554, 620, 665, 684, 706	Satlantic, OCI-200
Above-water surface downwelling irradiance, E_s	400, 412, 443, 455, 490, 510, 532, 554, 564, 590, 625, 670, 684, 700	Satlantic OCR-507 irradiance sensors

temperature and salinity dependence of absorption by pure water (Pegau et al., 1997) using temperature and salinity data measured with Hydrolab Datasonde 4a. Particulate scattering, $b_p(\lambda,z)$, was estimated as the difference between $c_{t-w}(\lambda,z)$ and $a_{t-w}(\lambda,z)$, after applying additional corrections to account for scattering losses manifested as overestimates of measured absorption (Kirk, 1992; Tzortziou et al., 2006). An ECOVSF3 instrument (WetLabs Inc.; Moore et al., 2000) that was calibrated annually was used to measure backscattering at three angles (100, 125, 150°) and three visible wavelengths (450, 530, 650 nm). Measurements were corrected for attenuation and were integrated (90–180°) to obtain total b_b according to Moore et al. (2000). Measurements by Boss et al. (2004) in the Case 2 waters off the coast of New Jersey showed that estimates of b_b using an ECOVSF were within 1.5% ($R^2 = 0.99$) of the b_b measured using a HOBILabs Hydroscat-6 (Maffione and Dana, 1997). Their results increase confidence on the accuracy of the backscattering measurements technique, especially since the instruments have large differences in design and calibration (Boss et al., 2004). Particulate backscattering was estimated as $b_{bp} = b_b - b_{bw}$, where b_{bw} is the backscattering of pure seawater estimated using a backscattering ratio of 0.5 and the seawater scattering coefficients, b_w, of Morel (1974) as retabulated by Smith and Baker (1981).

Water samples were collected from 4 to 5 depths at the four stations for analysis of IOPs and water quality. We used filtration to partition absorption among particulate and dissolved components. Particulate material was collected on 25 mm glass fiber filters (Whatman GF/F), while the filtrate passing a 0.22 μm pore-diameter membrane filter was used to measure absorption by colored dissolved organic matter (CDOM). Absorbance spectra were measured using a Cary-IV dual-beam spectrophotometer to estimate the contribution of phytoplankton, non-algal particulate matter, and CDOM to total light absorption, using the approach of Gallegos and Neale (2002). Absorbance spectra of the filters were corrected for scattering errors using a path-length amplification factor estimated empirically by comparing particulate optical density measured on filters and in particle suspension (Mitchell et al., 2000). Absorption spectral slope coefficients describing the exponential decrease of absorption with increasing wavelength for CDOM, S_{CDOM}, and non-algal particles, S_{nap}, were determined by applying non-linear exponential fits to the absorption coefficients vs wavelength (290–750 nm) (Blough and Del Vecchio, 2002). Chlorophyll-a concentration, [chl-a], was measured spectrophotometrically on 90% acetone extracts of seston collected on 47 mm GF/F glass fiber filters (Jeffrey and Humphrey, 1975).

3.3. Measurements of radiation fields

Two sensor arrays were used to measure underwater radiation fields, depending on instrument availability. On eight cruises underwater upwelling, $E_u(z)$, and downwelling, $E_d(z)$, spectral irradiance profiles, and above-water surface downwelling irradiance, E_s, were measured using Satlantic OCI-200 irradiance sensors (Table 1) that were calibrated annually. The sensors were mounted on a custom frame so that up- and down-welling sensors were nearly coplanar. For all other measurements of radiation fields we used a Satlantic MicroPro free-falling radiometer to measure water column profiles of upwelling radiance, $L_u(z)$, and $E_d(z)$, and Satlantic OCR-507 Surface Reference Irradiance sensors for measurements of E_s (Table 1). Measurements not meeting quality control (e.g. casts characterized by large tilt-angles or changing cloudiness conditions) were omitted from analysis. A correction was applied to the radiometric measurements through the instrument's calibration for the immersion effect (Satlantic, 2002). Measurements of $L_u(z)$ were corrected for the depth offset between the E_d and L_u sensors, and for self-shading (Gordon and Ding, 1992; Zibordi and Ferrari, 1995). The MicroPro instrument, used in our measurements of $L_u(z)$, has a smaller diameter (6.4 cm) and is less subject to instrument self-shading compared to other radiometric instruments (Harding and Magnuson, 2002).

For those cases when in-situ measurements of L_u were made, the water leaving radiance, L_w, was estimated by extrapolating $L_u(z)$ to just below the water surface $z = 0^-$ and estimating transmittance through the water–air interface. The upwelling radiance just below the water surface, $L_u(0^-,\lambda)$, was estimated through non-linear least squares fitting (SigmaStat software) of measured $L_u(z,\lambda)$ to the equation $L_u(z,\lambda) = L_u(0^-,\lambda)\ \exp(-K_{Lu}\cdot z)$, where K_{Lu} is the diffuse attenuation coefficient for the upwelling radiance, to a good approximation constant in the 0–3 m layer used in the regressions. The coefficients of determination (R^2 values) for the non-linear exponential fits were in most cases better than 0.99. To estimate L_w, we calculated the propagation of $L_u(0^-,\lambda)$ through the water–air interface:

$$L_w(\lambda,\theta,\varphi) = L_u\left(0^-,\lambda,\theta',\varphi\right)\frac{(1-r(\theta',\theta))}{n_w^2} \quad (2)$$

where θ' is the direction of the upward traveling photons incident from the water body onto the water surface, θ is the direction of the transmitted photons, $r(\theta',\theta)$ is the Fresnel reflectance for the associated directions θ' and θ, and n_w is the index of refraction of water ($n_w \approx 1.34$) (Mobley, 1994). For the geometry of our measurements, the zenith angle of water-leaving radiance and the nadir angle of in-water upward radiance are zero ($\theta' = \theta = 0$) and the transmittance is ($1 - r(\theta',\theta) \approx 0.98$ (Mobley, 1994). Therefore, $L_w(\lambda)$ can be estimated from Eq. (2) as:

$$L_w(\lambda) = 0.544 L_u\left(0^-,\lambda\right) \quad (3)$$

For those cases when in-situ measurements of L_u profiles were not available we estimated L_w from our in-situ measurements of IOPs (i.e. a, b, c, b_b) using the extensively validated Hydrolight underwater radiative transfer program (Mobley et al., 1993). Tzortziou et al. (2006) discussed the details of radiative transfer model calculations using Hydrolight for these Case 2 waters. Very good agreement (average absolute differences less than 10%) between L_w estimated based on Eq. (3) (using measured $L_u(z)$) and L_w estimated by Hydrolight

(using measured IOPs) demonstrated the consistency between data and model results and the very good optical closure between independently measured quantities (Tzortziou et al., 2006).

Based on its definition, $R_{rs}(\lambda)$ was estimated as the ratio of $L_w(\lambda)$ to measured $E_s(\lambda)$. Eq. (1), measured IOPs (i.e. a, b_b), and estimated R_{rs} were then used to examine variability in the quantity f/Q.

3.4. MODIS chlorophyll algorithms and products

The applicability of the three MODIS chlorophyll algorithms described below was examined for the studied region of the Chesapeake Bay:

(i) The SeaWiFS-analog OC3M chlorophyll algorithm (currently operational MODIS level-2 standard chlorophyll product 'Chlor-a') is an empirical algorithm (3rd order polynomial) that relates the greater of the ratios $R_{rs}(443)/R_{rs}(551)$ or $R_{rs}(488)/R_{rs}(551)$ to [chl-a] (O'Reilly et al., 2000).

(ii) The MODIS empirical-HPLC algorithm ('chlor_MODIS' product), is based on an empirical 3rd order polynomial derived from high performance liquid chromatography (HPLC) measurements of [chl-a] and blue:-green water reflectance ratios ($R_{rs}(443)/R_{rs}(551)$ and $R_{rs}(488)/R_{rs}(551)$) in Case 1 and Case 2 waters (Clark, 1997; updated 19 Feb. 2002, D. Clark, personal communication). The algorithm uses different polynomial constants for waters with high and low [chl-a]. A recently proposed version of the algorithm (updated 19 March 2003, D. Clark, personal communication) is a 5th order polynomial, expected to perform better in very high and very low [chl-a] environments.

(iii) The MODIS semi-analytical chlorophyll algorithm ('chlor_a_3' product) is based on a bio-optical model that relates R_{rs} to backscattering and absorption by phytoplankton and gelbstoff (combined term for CDOM and non-algal particles). However, for $a_{phyt}(675)$ larger than 0.03 m^{-1}, or [chl-a] higher than 1.5–2.0 mg m^{-3}, the MODIS semi-analytical algorithm automatically switches to an empirical relationship (3rd order polynomial) between [chl-a] and the ratio $R_{rs}(488)/R_{rs}(551)$ (Carder et al., 2002). The polynomial constants are adjusted dynamically (based on information on the sea surface temperature) in order to account for pigment packaging effects ('packaged', 'un-packaged', and transitional cases) in nutrient-replete and nutrient-deplete conditions.

In summary, when applied to waters with [chl-a] larger than ~2 mg m^{-3}, which is typically the case in coastal waters like Chesapeake Bay, all three MODIS algorithms are based on empirical relationships between [chl-a] and R_{rs} ratios at blue:-green wavelengths. To examine the performance of the MODIS algorithms in the studied region of the Bay we applied the satellite algorithms to R_{rs} spectra estimated from our in-situ bio-optical data. We then compared these [chl-a] estimates to measured surface [chl-a] values.

4. Results

4.1. Water optical characteristics

Water bio-optical characteristics showed large spatial and temporal variability. Relatively clear waters were observed during the fall cruises, with low biological activity and relatively low total absorption, total attenuation and chlorophyll concentration values. Higher chlorophyll concentrations, associated with large surface phytoplankton bloom events, were observed in spring and summer (Tzortziou, 2004). Surface [chl-a] values ranged from 3.5 mg m^{-3} (station PI, 13 November 2001) to 74 mg m^{-3} (station HB, 11 June 2001) with an average value of 14.7 mg m^{-3} (Fig. 2).

Non-covarying CDOM and non-algal particles (R^2 between 0.01 and 0.28 for the regressions among a_{phyt}, a_{CDOM}, and a_{nap} at 440 nm, $N = 137$) contributed considerably to light attenuation at the blue wavelengths used in the MODIS chlorophyll retrievals. Combined contribution by CDOM and non-algal particles to surface (0–1 m) a_{t-w} was on average 59% at 488 nm (average $a_{t-w}(488)$ of 0.75 m^{-1}, SD = 0.55 m^{-1}). Absorption by non-algal particles alone was on average 41% of a_{t-w} at 488 nm, getting as large as 56% of $a_{t-w}(488)$ at the highly turbid station JT on 9 July 2001. Contribution by CDOM and non-algal particles to surface a_{t-w} was even larger at shorter wavelengths (e.g. 73% at 412 nm) because of the exponential increase in the absorption of both substances with decreasing wavelength. Estimated S_{CDOM} averaged 0.018 nm^{-1} (SD = 0.0032 nm^{-1}) and S_{nap} averaged 0.011 nm^{-1} (SD = 0.001 nm^{-1}).

Large spatial and temporal variation was observed in particulate backscattering, with surface $b_{bp}(530)$ ranging between 0.013 and 0.166 m^{-1}. Higher b_{bp} values were observed consistently at the near shore site JT, compared to the other three

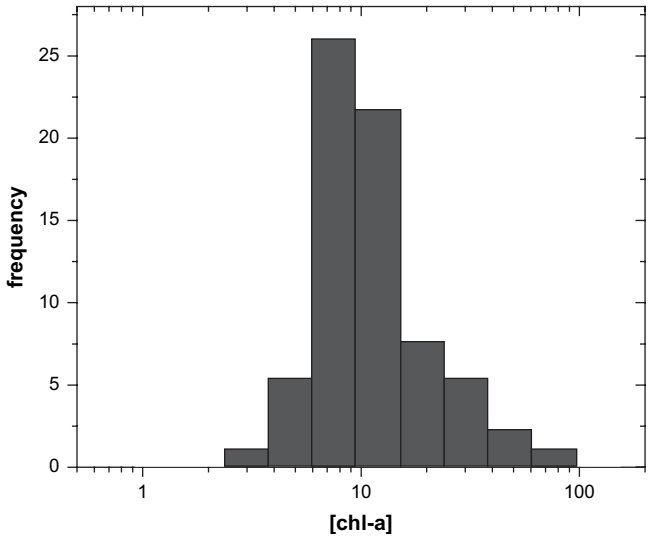

Fig. 2. Frequency histogram of surface [chl-a] (mg m^{-3}) measured during our cruises in the mid Chesapeake Bay, 2001–2002.

stations. Particulate backscattering fraction values, b_{bp}/b_p, ranged from 0.006 to 0.036 at 530 nm, with the largest b_{bp}/b_p value of 0.036 occurring close to the bottom at station JT. The b_{bp}/b_p values, averaged over all depths at the four stations, were 0.0133 (SD = 0.0032), 0.0128 (SD = 0.0032), and 0.0106 (SD = 0.0029), at 450, 530 and 650 nm, respectively. Surface b_{bp}/b_p at 530 nm, estimated from measurements within 1 m from the surface, had an average value of 0.0125 (SD = 0.003) at the four stations. Surface $b_{bp}/b_p(530)$ was typically higher at station JT, with an average value of 0.0146 (SD = 0.0037).

Observed variability in water IOPs resulted in large spatial and temporal variability in the magnitude of measured R_{rs} spectra. However, in all cases, maximum values of R_{rs} occurred in the green (i.e. 554 nm, Fig. 3) because of the large pure-water absorption in the red and the large CDOM and non-algal particulate absorption in the blue region of the spectrum.

4.2. MODIS chlorophyll-a algorithm performance

Since chlorophyll concentrations were consistently higher than 3.5 mg m^{-3}, all MODIS chlorophyll retrievals were based on empirical relationships between [chl-a] and blue:green R_{rs} ratios. There was poor agreement between measured surface [chl-a] and [chl-a] values estimated by applying the MODIS algorithms to R_{rs} spectra derived from our in-situ bio-optical data for all satellite algorithms (Fig. 4). The root mean square of the relative differences, RMSrd, between model and measured [chl-a] ranged between 54 and 92% (Fig. 4; $N = 40$). For some chlorophyll algorithms this value was larger than the RMSrd between measured [chl-a] and the average [chl-a] measured in these waters (74%), suggesting that in these cases the average measured [chl-a] was a better predictor than the algorithm.

We then examined the correlation between surface [chl-a] and two-band R_{rs} ratios at various MODIS wavebands (Table 2). Consistent with the weak performance of MODIS chlorophyll algorithms in these waters, we observed relatively weak correlation between measured $\log_{10}$([chl-a]) and blue:green R_{rs} ratios (R^2 less than 0.39; Table 2). The strongest correlation was found between [chl-a] and the ratio $R_{rs}(677)/R_{rs}(554)$ ($R^2 = 0.54$). The empirical relationship found between [chl-a] and this R_{rs} ratio was consistent with expectations based on our in-situ bio-optical data (Tzortziou, 2004). Based on Eq. (1), and assuming $f/Q \cdot (t_{w-a} \cdot t_{a-w})/n_w^2$ independent of wavelength and $b_b \ll a$, the ratio $R_{rs}(677):R_{rs}(554)$ is proportional to the backscattering ratio and inversely proportional to the absorption ratio at these two wavelengths (i.e. $R_{rs}(677)/R_{rs}(554) = b_b(677)/b_b(554) \cdot a(554)/a(677)$). For the studied region of the Bay, b_b in the green was strongly correlated with b_b in the red ($R^2 = 0.99$; Table 2). Strong correlation and linear relationship ($R^2 = 0.92$) was also found between $a_{t-w}(554)$ and $a_{t-w}(677)$ based on our AC-9 data (Table 2). Because phytoplankton is the major absorber (other than pure water) in the 677 nm wavelength region, absorption at 677 was expected to be strongly correlated with [chl-a], with some variation due to changes in phytoplankton species composition, physiological state, and size (Bricaud et al., 1995). Indeed, least squares regression for our data gave: $a_{t-w}(677) = 0.0166 \cdot$ [chl-a] + 0.0603 ($R^2 = 0.92$; Table 2), with the small intercept due to the small, residual absorption by CDOM and non-algal particulate matter at 677 nm. Including the effect of chlorophyll fluorescence at 677 nm using detailed radiative transfer model calculations (Tzortziou, 2004), we found that the relationship observed between [chl-a] and $R_{rs}(677)/R_{rs}(554)$ was consistent with predictions based on independently derived relationships between [chl-a] and the ratio of measured IOPs (i.e. b_b, a) at the two specific wavelengths.

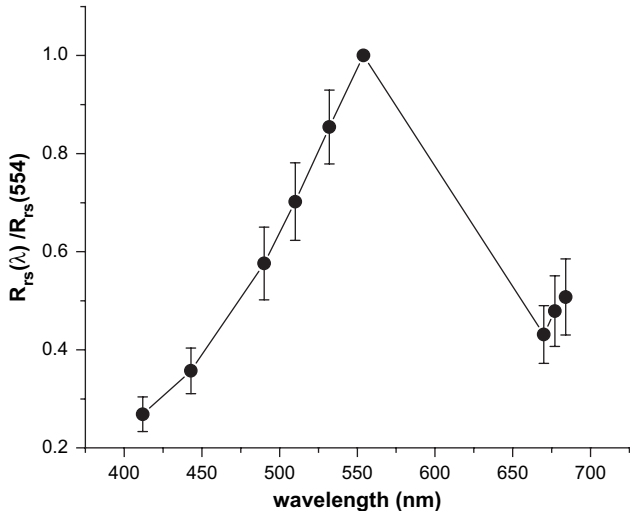

Fig. 3. Average R_{rs} spectrum for the mid Chesapeake Bay waters, estimated after normalizing individual R_{rs} spectra to R_{rs} at 554 nm ($N = 44$). Standard deviation is shown as y-error bars.

4.3. Observed variability in f/Q

We examined the relationship between $R_{rs}(\lambda)$ and the ratio of IOPs $b_b(\lambda)/(a(\lambda) + b_b(\lambda))$ using our estimates of R_{rs} and in-situ data of surface $b_b(\lambda)$ and $a(\lambda)$ to: (i) assess variability in the quantity f/Q (based on Eq. (1)) for the nadir-viewing geometry of our measurements, and (ii) compare our observations for these Case 2 waters with previous theoretical studies on f/Q variability for same viewing geometry but Case 1 waters (Morel and Mueller, 2002).

R_{rs} values at 443, 532 and 670 nm were strongly correlated with $b_b/(a + b_b)$ at all three wavelengths, whether R_{rs} was calculated from measured L_u and E_s using Eq. (3) (Fig. 5, solid circles) or estimated from measured IOPs using the radiative transfer model (Fig. 5, open circles). Coefficients of determination (R^2 values) were larger than 0.92 in all cases.

$(f/Q) \cdot (t_{(w,a)} t_{(a,w)}/n_w^2)$ values estimated as the slope of the linear least square regression of the pooled dataset of R_{rs} versus $b_b/(a + b_b)$ ranged from 0.0491 to 0.058 sr^{-1} for the three different wavelengths, with coefficients of variation in the estimated slopes less than 1.4% ($N = 37$). Very similar results were obtained when R_{rs} values estimated from the two

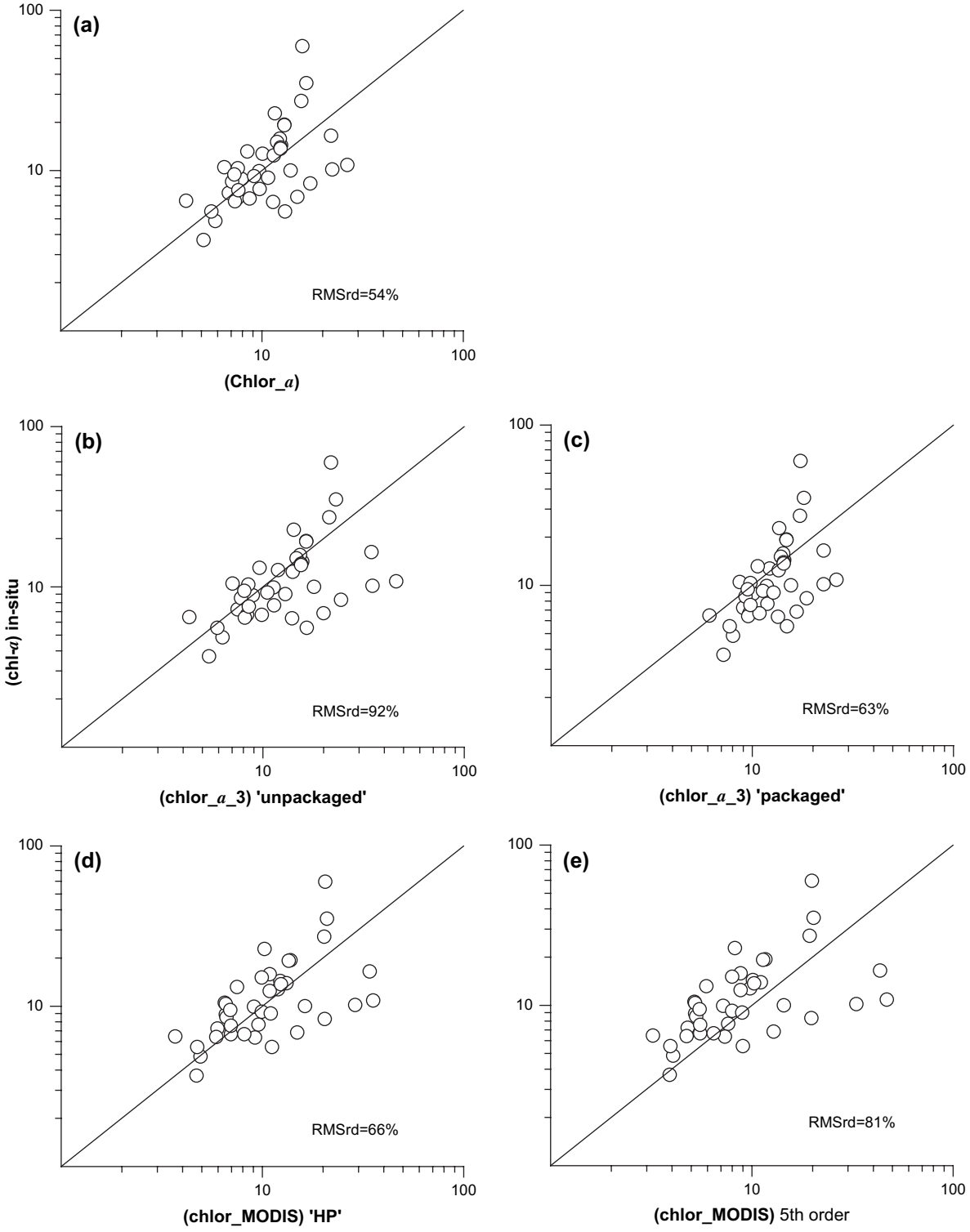

Fig. 4. Comparison between measured surface [chl-a] (mg m^{-3}) and [chl-a] values estimated after applying the MODIS algorithms to R_{rs} spectra derived from our in-situ bio-optical data (1:1 line shown for reference). The MODIS chl-algorithms used were: (a) ''Chlor_a'', (b) 'chlor_a_3' for the 'unpackaged' case, (c) 'chlor_a_3' for the 'fully packaged' case, (d) 'chlor MODIS' for the high chl-a pigment (always the case for our data), and (e) 'chlor MODIS', 5th order polynomial. The root mean square of the relative differences, RMSrd, between model and measured [chl-a] is shown for each case. The RMSrd between measured [chl-a] and the average [chl-a] measured in these waters was 74%.

different methods (using measured L_u, or measured IOPs and radiative transfer calculations) were treated separately, as expected based on the results of good optical closure reported by Tzortziou et al. (2006).

Essentially identical values were obtained by averaging all R_{rs}: $b_b/(a + b_b)$, suggesting that the modeled f/Q (i.e. slope in the regression R_{rs} vs $b_b/(a + b_b)$) represented well the individual measurements (i.e. individual R_{rs}: $b_b/(a + b_b)$ ratios) over

Table 2
Regression relationships between IOPs and R_{rs} in the mid Chesapeake Bay

Parameters (Y vs X)	Regression relationship	R^2
$R_{rs}(412)/R_{rs}(554)$ vs [chl-a]	$\log_{10}(Y) = -0.1261 \cdot \log_{10}(X) - 0.4508$ ($N = 40$)	0.24
$R_{rs}(443)/R_{rs}(554)$ vs [chl-a]	$\log_{10}(Y) = -0.1537 \cdot \log_{10}(X) - 0.2933$ ($N = 40$)	0.39
$R_{rs}(488)/R_{rs}(554)$ vs [chl-a]	$\log_{10}(Y) = -0.1299 \cdot \log_{10}(X) - 0.1074$ ($N = 40$)	0.32
$R_{rs}(510)/R_{rs}(554)$ vs [chl-a]	$\log_{10}(Y) = -0.1168 \cdot \log_{10}(X) - 0.0339$ ($N = 40$)	0.36
$R_{rs}(532)/R_{rs}(554)$ vs [chl-a]	$\log_{10}(Y) = -0.0728 \cdot \log_{10}(X) + 0.0068$ ($N = 40$)	0.23
$R_{rs}(670)/R_{rs}(554)$ vs [chl-a]	$\log_{10}(Y) = 0.166 \cdot \log_{10}(X) - 0.5467$ ($N = 40$)	0.48
$R_{rs}(677)/R_{rs}(554)$ vs [chl-a]	$\log_{10}(Y) = 0.1725 \cdot \log_{10}(X) - 0.5117$ ($N = 40$)	0.54
$a_{t-w}(677)$ vs [chl-a]	$Y = 0.0166 \cdot X + 0.0603$ ($N = 137$)	0.92
$a_{t-w}(554)$ vs $a_{t\text{-}w}(677)$	$Y = 0.68 \cdot X + 0.08$ ($N = 156$)	0.92
$b_b(650)$ vs $b_b(530)$	$Y = 0.74 \cdot X$ ($N = 677$)	0.99
$R_{rs}(443)$ vs $\frac{b_b(450)}{a_w(440) + a_{t-w}(440) + b_b(450)}$	$Y = 0.0491 \cdot X$ ($N = 37$)	0.92
$R_{rs}(532)$ vs $\frac{b_b(530)}{a_w(532) + a_{t-w}(532) + b_b(530)}$	$Y = 0.0519 \cdot X$ ($N = 37$)	0.95
$R_{rs}(670)$ vs $\frac{b_b(650)}{a_w(670) + a_{t-w}(670) + b_b(650)}$	$Y = 0.058 \cdot X$ ($N = 37$)	0.96
$b_b(450)$ vs $R_{rs}(443)$	$Y = 34.06 \cdot X - 0.02$ ($N = 37$)	0.67
$b_b(530)$ vs $R_{rs}(532)$	$Y = 12.63 \cdot X - 0.017$ ($N = 37$)	0.77
$b_b(650)$ vs $R_{rs}(670)$	$Y = 15.82 \cdot X - 0.008$ ($N = 37$)	0.88
$b_b(650)$ vs $a_{nap}(412)$	$Y = 0.0463 \cdot X - 0.0092$ ($N = 44$)	0.76
$b_b(650)$ vs $a_{nap}(380)$	$Y = 0.0411 \cdot X - 0.0107$ ($N = 44$)	0.83
[chl-a] vs $b_b(650)$	$Y = 354 \cdot X + 2.10$ ($N = 44$)	0.42
$a_{nap}(412)$ vs $R_{rs}(670)$	$Y = 302.2 \cdot X + 0.159$ ($N = 33$)	0.70
$a_{nap}(380)$ vs $R_{rs}(670)$	$Y = 356.71 \cdot X + 0.168$ ($N = 33$)	0.74

the whole range of conditions. No strong correlation was found between $(f/Q) \cdot (t_{(w,a)} t_{(a,w)} / n_w^2)$ and solar zenith angle for our measurements (R^2 less than 0.06).

4.4. Relationships between b_b, particulate matter, and R_{rs}

Regression of R_{rs} on b_b was used to examine the effect of particulate backscattering on R_{rs} over the wide range of in-water optical characteristics (Fig. 6a–c). R_{rs} at 670 nm was strongly correlated with surface b_b at 650 nm (Fig. 6c) ($R^2 = 0.88$). Correlation between R_{rs} and b_b was statistically significant but not as strong at the shorter wavelengths (i.e. $R_{rs}(443)$ versus $b_b(450)$ in Fig. 6a with $R^2 = 0.67$, and $R_{rs}(532)$ versus $b_b(530)$ in Fig. 6b with $R^2 = 0.77$).

Variability in $R_{rs}(670)$ was mainly driven by changes in b_b (and not as much by changes in a) because of the relatively large contribution by pure water to total absorption at 670 nm. Surface b_b in the red ranged between 0.008 and 0.13 m^{-1} during our measurements in the Bay. This variability in backscattering, by more than an order of magnitude, corresponds to more than an order of magnitude changes in $R_{rs}(670)$ (based on Eq. (1)). R_{rs} is also affected by changes in total in-water absorption. However, when $a_{t-w}(670)$ (observed range 0.1–1 m^{-1}) is added to the relatively large pure water absorption ($a_w(670) = 0.44$ m^{-1}; Pope and Fry, 1997) total absorption varies by less than a factor of 3. At shorter visible wavelengths, the contribution of pure water absorption is minimal. Therefore, R_{rs} at 443 and 532 nm is affected strongly by changes in both total absorption (strong contribution by non-covarying particulate and dissolved components) and total backscattering (contribution by suspended particles).

To examine the relative contribution of algal and non-algal particles to b_b variability in these waters, we applied linear regressions between surface b_b and [chl-a], and between b_b and a_{nap} (proxy for non-algal particle abundance). Backscattering at all three wavelengths 450, 530 and 650 nm (only $b_b(650)$ nm shown in Fig. 7) was strongly correlated with the particularly strong absorption by non-algal particles in the blue (e.g. 412 nm) and UV (e.g. 380 nm) ($R^2 = 0.83$ for the linear least-square regression $b_b(650)$ vs $a_{nap}(380)$). The relationship between surface [chl-a] and surface b_b was highly variable at all three wavelengths (only 650 nm shown in Fig. 8) and correlation was considerably smaller ($R^2 = 0.42$) compared to that between b_b and a_{nap}.

Given the strong correlation between $R_{rs}(670)$ and $b_b(650)$, and between $b_b(650)$ and a_{nap}, a strong correlation would be expected between $R_{rs}(670)$ and absorption by non-algal particles. Indeed, coefficients of determination for the linear least-squares regression between $R_{rs}(670)$ and surface a_{nap} were 0.7 and 0.74 for absorption measurements at 412 and 380 nm, respectively (Fig. 9, Table 2).

5. Discussion

Obtaining accurate information on the composition and concentration of dissolved and particulate, organic and inorganic matter in near shore waters using remotely sensed ocean color is critical for primary production studies, coastal water quality monitoring, and carbon cycling modeling. However,

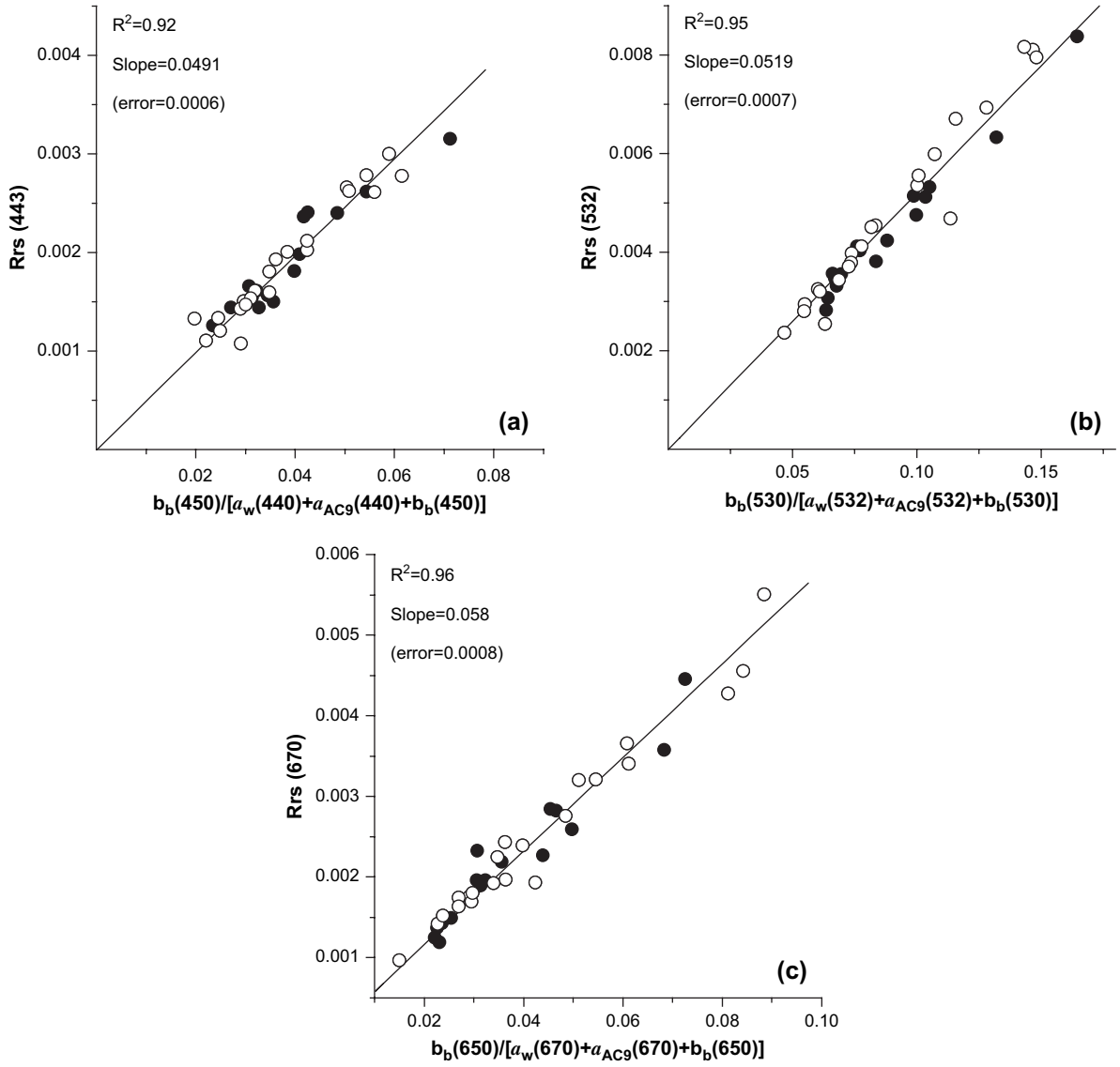

Fig. 5. Relation between $R_{rs}(\lambda)$ (sr^{-1}) and $b_b(\lambda)/(a(\lambda)+b_b(\lambda))$, for R_{rs} calculated from measured L_u and E_s using Eq. (3) (solid circles) and R_{rs} estimated from measured IOPs using Hydrolight (open circles), at (a) 443 nm, (b) 532 nm and (c) 670 nm. Linear least-squares regression fits applied to the pooled dataset of R_{rs} vs $b_b(\lambda)/(a(\lambda)+b_b(\lambda))$ are shown as solid lines (R^2 between 0.92 and 0.96; $P < 0.0001$ in all cases). Regression results are summarized in Table 2.

application of currently operational satellite algorithms in near shore waters like the Chesapeake Bay often results in erroneous retrievals, as shown here for the MODIS chlorophyll algorithms. Effective remote retrieval of biogeochemical variables in coastal waters depends to a large extent on the accuracy of, and consistency among, the in-situ data used in the development, validation, and improvement of the applied remote sensing bio-optical algorithms. Thus, the degree of closure among bio-optical quantities independently measured in the field becomes critical for remote sensing applications. Previously, we reported close agreement between data and radiative transfer model results over a wide range of conditions in mid Chesapeake Bay, and demonstrated very good optical closure between independently measured quantities (Tzortziou et al., 2006). These results increased confidence in the accuracy of, and consistency among, our in-situ bio-optical data.

5.1. MODIS chlorophyll-a algorithm performance

Chlorophyll concentrations larger than 2 mg m^{-3} are typically observed in the mid and upper Chesapeake Bay (e.g. Magnuson et al., 2004) and our measured [chl-a] ranged between 3.5 and 74 mg m^{-3}. For [chl-a] $>$ 2 mg m^{-3} all MODIS chlorophyll retrievals are based on empirical relationships between [chl-a] and blue:green reflectance ratios. When we applied these algorithms to our estimates of R_{rs} to examine the MODIS algorithm performance in the studied region of the Bay, we found large disagreement between estimated and measured surface [chl-a] (Fig. 4). The weak performance of MODIS chlorophyll retrievals in these Case 2 waters is not surprising considering our results showing large contribution by non-covarying CDOM and non-algal particles to total light absorption in the blue. The MODIS algorithms do not sufficiently account

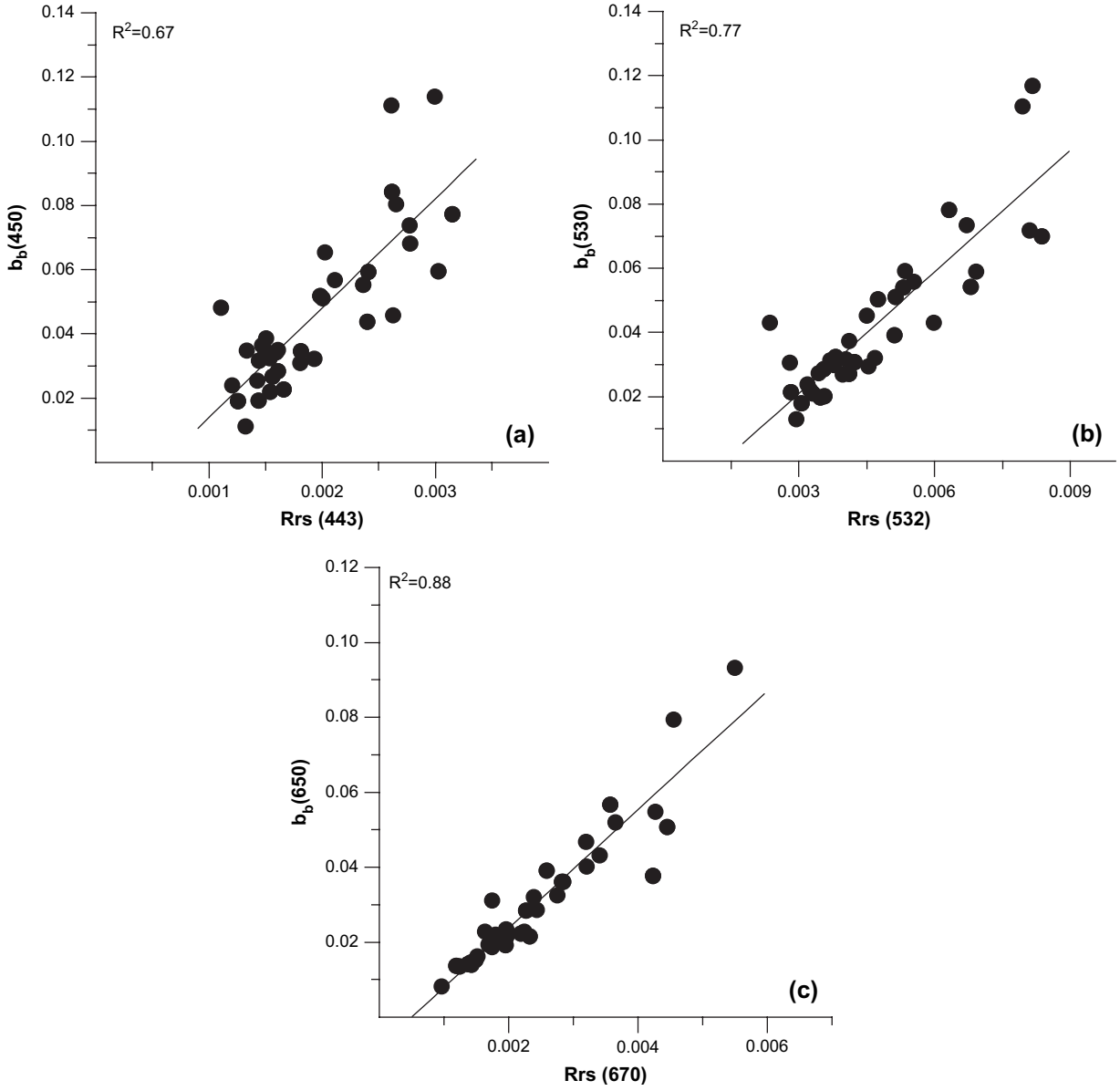

Fig. 6. Relation between measured b_b (m^{-1}) and R_{rs} (sr^{-1}) at wavelengths (a) 443 nm (b_b measured at 450 nm), (b) 532 nm (b_b measured at 530 nm) and (c) 670 nm (b_b measured at 650 nm) (R^2 and N are given in Table 2).

for this large interference from CDOM and non-algal particulate absorption. Our results are consistent with findings by Harding et al. (2005) who examined the performance of the SeaWiFS empirical chlorophyll algorithm OC4v4 in the Chesapeake Bay. The OC4v4 chlorophyll algorithm is the SeaWiFS ''analog'' of the currently default MODIS algorithm OC3M examined here. Wozniak and Stramski (2004) used Mie scattering calculations to show that even relatively low concentrations of mineral particles of the order of 0.1 g m^{-3} can considerably affect chlorophyll estimations from standard SeaWiFS and MODIS algorithms that are based on blue:green reflectance ratios. In near-shore, estuarine waters like Chesapeake Bay, mineral particulate concentrations are typically much larger (average concentration of 4.8 g m^{-3} measured during our cruises; unpublished data, C. Gallegos), strongly affecting the R_{rs} signal in the blue-green.

Because of the strong interference from CDOM and non-algal particulate absorption in the blue-green, regionally specific algorithms based on the strong chlorophyll-a fluorescence signal at around 685 nm or the chlorophyll-a absorption feature at 675 nm have been proposed for improving chlorophyll retrievals in highly turbid, coastal and inland waters (e.g. Gower et al., 1984; Gons, 1999; Ruddick et al., 2001; Dall'Olmo et al., 2005). When we examined correlation between [chl-a] and various MODIS R_{rs} ratios using our in-situ data we found that variability in surface [chl-a] was most strongly correlated with changes in $R_{rs}(677)/R_{rs}(554)$ (Table 2). The derived relationship between [chl-a] and this R_{rs} ratio was consistent with predictions based on radiative transfer calculations and observed relationships between in-situ data of [chl-a] and IOPs (b_b and a) at the two specific wavelengths.

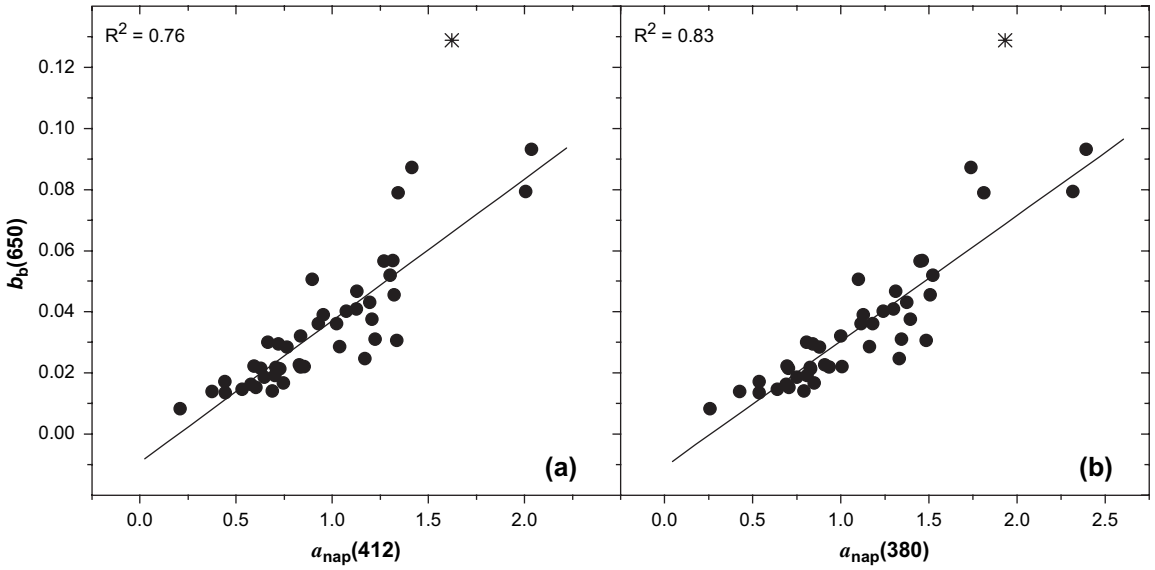

Fig. 7. Relation between surface measurements of $b_b(650)$ (m^{-1}) and a_{nap} (m^{-1}) at (a) 412 nm and (b) 380 nm (R^2 and N are given in Table 2). One of the datapoints (shown as an asterisk) was obtained under phytoplankton bloom conditions (station HB, 11 June 2001) and, thus, was not included in the regressions.

These results are the first step towards the development of regionally specific chlorophyll algorithms for the Chesapeake Bay using remotely sensed ocean reflectance in the red. Moreover, one of the main factors affecting the accuracy of satellite chlorophyll retrievals in near shore waters is correction for the atmosphere's optical characteristics. Problems with atmospheric correction of satellite data in the blue due to extrapolation of aerosol properties from near-infrared to shorter wavelengths (Gordon and Voss, 1999) are avoided when using information in the red wavelengths for chlorophyll retrievals. The relationships found here between [chl-a] and various R_{rs} ratios for the Chesapeake Bay strongly suggest that exploiting the ocean color signal in the red, where interference from CDOM and non-algal particulate absorption is minimal, is necessary for improving satellite monitoring of biological activity in these Case 2 waters.

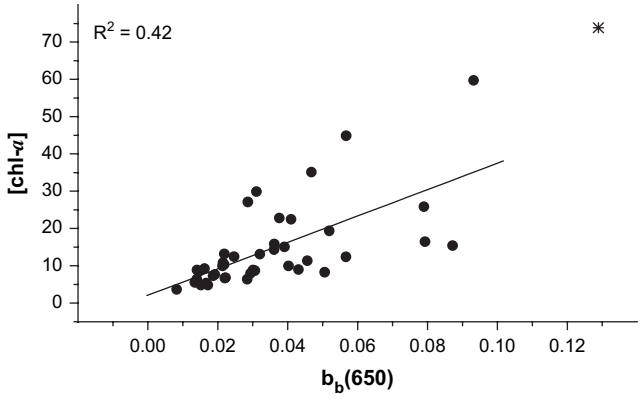

Fig. 8. Relation between measured surface [chl-a] (mg m^{-3}) and surface $b_b(650)$ (m^{-1}) (R^2 and N are given in Table 2). One of the datapoints (shown as an asterisk) was obtained under phytoplankton bloom conditions (station HB, 11 June 2001) and, thus, was not included in the regression.

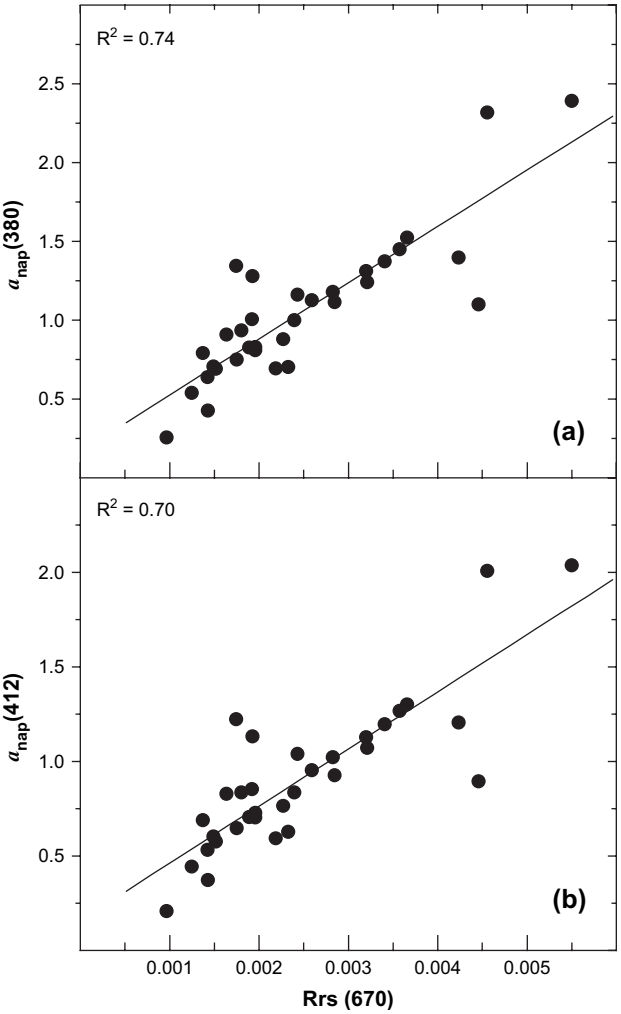

Fig. 9. Linear regression between $R_{rs}(670)$ (sr^{-1}) and surface measurements of absorption by non-algal particles (m^{-1}) at (a) 380 nm and (b) 412 nm (R^2 and N are given in Table 2).

5.2. R_{rs}, IOPs, and variability in f/Q

Since R_{rs} is related to the backscattering and absorption properties of all the optically significant water constituents, approximate forms of Eq. (1) have commonly been used in the development of semi-analytical bio-optical models for remote retrieval of surface [chl-a] and IOPs in Case 2 waters. Such approximations are often based on the assumption that the quantity f/Q is independent of wavelength, or in-water and air–water boundary conditions (e.g. semi-analytic version of chlorophyll algorithm by Carder et al., 2002; Gordon et al., 1988). However, recent model results by Morel and Mueller (2002) for vertically homogeneous, Case 1 waters, suggest that variations in f/Q (due to its dependence on water IOPs and illumination conditions) are within the range 0.08–0.15 sr^{-1}.

Our detailed measurements of b_b, a, and R_{rs} spectra allowed us to examine the relationship between R_{rs} and the IOPs ratio $b_b/(a+b_b)$, and assess observed variability in the quantity f/Q for the nadir-viewing geometry of our measurements in the studied region of the Chesapeake Bay. Close agreement in the resulting relationships between $b_b/(a+b_b)$ and R_{rs}, whether R_{rs} was estimated based on measured L_u (using Eq. (3)) or based on measured IOPs (using Hydrolight) was consistent with the good optical closure demonstrated by Tzortziou et al. (2006) for these Case 2 waters. Estimated values of $(f/Q)\cdot(t_{(w,a)}t_{(a,w)}/n_w^2)$, derived from the linear regression of R_{rs} versus $b_b/(a+b_b)$ (Fig. 5), ranged from 0.0491 to 0.058 sr^{-1}. Very similar results were derived by averaging individual ratios. Since $t_{(a,w)}t_{(w,a)}/n_w^2$ is approximately 0.54 (Mobley, 1994), these results correspond to f/Q values in the range 0.09–0.107 sr^{-1}. Interestingly, the range of f/Q values we derived for the Case 2 Chesapeake Bay waters is very similar to the range of f/Q values (0.08–0.11 sr^{-1}) reported by Morel and Mueller (2002) in their theoretical computations for same geometry of measurements (nadir-viewing) but Case 1 waters (their Fig. 13.10).

Our measurements in the Bay were performed over a wide range of water bio-optical characteristics (e.g. [chl-a] in the range 3.5–74 mg m^{-3}), at different solar zenith angles (θ_o between 16° and 58°), and for both hazy and clear atmospheric conditions. However, the standard deviation of the f/Q values estimated from individual datasets of R_{rs}: $b_b/(a+b_b)$ was less than 10%, and coefficients of variation in the estimated slopes of the linear regressions between R_{rs} and $b_b/(a+b_b)$ (average f/Q over a range of conditions) were less than 1.4%. These results suggest that for the nadir viewing geometry of our measurements in these Case 2 waters observed variability in the quantity f/Q was not very large and not considerably different from Case 1 waters.

5.3. R_{rs}, backscattering and particulate matter

As the spectral reflectance of the ocean is to a first approximation proportional to $b_b/(a+b_b)$, backscattering processes are of primary importance to applications of optical remote sensing in oceanography. Backscattering signal depends on the concentration, composition, size distribution, shape, and refractive index of suspended, organic and inorganic, marine particles (van de Hulst, 1981). Thus, b_b carries useful information about seawater constituents that affect biological activity, biogeochemical cycling, and carbon fluxes in coastal ecosystems. Carbon content in individual plankton cells has been found to be related to particle size (e.g. Verity et al., 1992; Montagnes et al., 1994) and refractive index (Stramski, 1999). Measurements by Stramski et al. (1999) in the Southern Ocean revealed high correlation between surface particulate backscattering at 510 nm and surface concentration of particulate organic carbon (POC). In coastal waters a significant fraction of suspended particulate matter consists of highly refractive, inorganic mineral particles, derived from coastal erosion, river discharge of terrigenous inorganic particles, bottom resuspension, or aeolian inputs (Stramski et al., 2004). In coastal waters therefore, strong correlation between backscattering and POC is not to be expected.

Variation in particulate backscattering in the studied region of the Chesapeake Bay can be related to variations in particulate loading, mixing, and distance off-shore. Highly backscattering waters were observed near station JT, which is located closest to the land among the four sampling stations and is more strongly influenced by shoreline erosion and resuspension of bottom sediments due to tidal and land boundary effects (Fig. 1). Variation in surface b_b significantly affected R_{rs} at all wavelengths (Fig. 6), and was found to be the main factor driving observed variability in the R_{rs} at 670 nm (Fig. 6c). The strong correlation found between b_b and $R_{rs}(670)$ indicates that satellite measured R_{rs} at 670 nm can be applied to remotely retrieve particulate backscattering in these Case 2 waters.

Estimated particulate backscattering fraction in the Chesapeake Bay had an average value of ~0.013 at 530 nm, in agreement with b_b/b values reported by Sydor and Arnone (1997) for the near shore waters off Mississippi. The observed spectral shape of b_b/b is in agreement with Mobley et al. (2002) who measured a decrease in b_b/b from 442 to 555 nm by less than 24%, for the Case 2 waters offshore of New Jersey. Backscattering fraction can provide a proxy to the particulate bulk refractive index, which in turn is an indicator of the particulate composition in the water (Twardowski et al., 2001; Sullivan et al., 2002; Stramski et al., 2004). Due to their high water content phytoplankton cells have relatively low refractive index compared to inorganic particles (e.g. Carder et al., 1974; Aas, 1981, 1996; Stramski et al., 1988). As particulate backscattering increases with increasing particulate refractive index, b_{bp}/b_p values for phytoplankton-dominated waters are typically lower than those of waters where suspended inorganic particles and detrital material dominate (Twardowski et al., 2001; Sullivan et al., 2002). Measurements by Twardowski et al. (2001) in the Gulf of California and Boss et al. (2004) off the New Jersey coast showed that phytoplankton-dominated surface waters with high chlorophyll concentrations had b_{bp}/b_p values of ~0.005–0.006, while b_{bp}/b_p was higher (exceeding 0.012

according to Boss et al., 2004) in regions where highly refractive re-suspended inorganic particles dominated. In agreement with these studies, we observed the largest b_{bp}/b_p values (b_{bp}/b_p of 0.025–0.036) close to the bottom at station JT, consistent with a higher proportion of re-suspended inorganic sediments in bottom waters. Surface b_{bp}/b_p (530) at the four stations sampled had an average value of 0.0125. This is considerably larger than the b_{bp}/b_p of phytoplankton-dominated waters (e.g. Twardowski et al., 2001; Boss et al., 2004). These results, and the even higher (average of 0.0146) surface b_{bp}/b_p measured at the highly turbid station JT, suggest that particulate backscattering in mid Chesapeake Bay surface waters is dominated by suspended non-algal particles, such as highly refractive minerals or organic detritus with low water content (Twardowski et al., 2001; Green et al., 2003).

The inference of qualitative geochemical information on non-algal particles from their optical characteristics (e.g. absorption magnitude and S_{nap}) is still a major challenge for effective remote sensing in coastal environments (e.g. Ferrari et al., 2003). The magnitude of non-algal particulate absorption in the studied region of the Bay showed strong seasonal and temporal variability, and weak covariation with CDOM or chlorophyll concentration (Tzortziou, 2004). However, there was little variation in the spectral shape of the non-algal particulate absorption, with S_{nap} values having a narrow range around an average of 0.011 nm^{-1} (SD = 0.001 nm^{-1}). Previous studies suggest that S_{nap} values of about 0.011 nm^{-1} are typical for mineral-dominated waters. Bowers et al. (1996) estimated an average S_{nap} value of 0.011 nm^{-1} (SD = 0.0002 nm^{-1}) for the absorption spectra of over 100 samples of mineral suspended solids collected from the Menai Strait in the Irish Sea. Measurements by Babin et al. (2003) at about 350 stations in European coastal waters showed that S_{nap} had an average value of 0.0117 nm^{-1} for the mineral-dominated waters in the North Sea and English Channel. Ferrari et al. (2003) measured S_{nap} values in the range 0.0095–0.0125 nm^{-1} for the coastal waters of the North Sea and German Bight where the main fraction of total suspended solids (76%) was inorganic. Relatively higher S_{nap} values, in the range 0.0115–0.0145 nm^{-1} were reported for the Baltic Sea, which is known for its high organic matter content (Voipo, 1981; Ferrari et al., 2003). Similarly, Babin et al. (2003) found that highly organic samples collected from the Baltic Sea had significantly higher S_{nap} values compared to mineral-dominated waters, suggesting that observed variation in S_{nap} may be related to the proportion of mineral and organic matter. The close agreement between our estimates of S_{nap} and those reported in other studies for suspended inorganic particles, and the large b_{bp}/b_p values we measured relative to phytoplankton-dominated waters, indicate that highly refractive non-algal particles with high inorganic content are the major water constituents controlling changes in both a_{nap} and b_{bp} in these Case 2 waters. Consistent with these results, we found that b_b, although highly variable, was strongly correlated with the magnitude of non-algal particulate absorption at 380 nm ($R^2 = 0.83$, Fig. 7).

The correlation between particulate b_b and a_{nap}, in conjunction with remote retrieval of surface b_b from $R_{rs}(670)$, suggest that $R_{rs}(670)$ can be applied to remotely determine abundance and distribution of non-algal particulate matter in near-shore regions where suspended inorganic particles strongly affect ocean color. For the Chesapeake Bay surface waters we showed that, indeed, $R_{rs}(670)$ is strongly correlated with non-algal particulate absorption at 380 nm (Fig. 9). Binding et al. (2003) found good correlation between surface irradiance reflectance ($R = E_u/E_d$) at 665 nm and concentration of mineral suspended sediments for the Irish Sea waters. Due to the similarity in the absorption spectral shapes of CDOM and non-algal particles, separating contribution by the two components to total light absorption in Case 2 waters is a difficult task. As a result, most satellite Case 2 algorithms (e.g. Maritorena et al., 2002; Magnuson et al., 2004), including the MODIS semi-analytical chlorophyll algorithm (Carder et al., 2002), combine CDOM and non-algal particles into one term (e.g. ''gelbstoff'') even though the two components do not covary in coastal waters. Regionally specific relationships, such as those we have derived here between $a_{nap}(380)$, $b_b(650)$, and $R_{rs}(670)$, allow a separate estimate of the contribution by non-algal particulate matter to total light absorption based on the backscattering properties of the non-algal particles and the remote retrieval of particulate b_b from satellite-measured R_{rs}.

6. Summary and conclusions

Effective interpretation of ocean color is a major challenge in near-shore Case 2 waters like the Chesapeake Bay. We found that relationships between [chl-a] and two-band R_{rs} ratios in the red-green wavelengths (i.e. $R_{rs}(677)/R_{rs}(554)$), where interference from CDOM and non-algal particulate absorption is minimal, provide a better basis for satellite monitoring of phytoplankton blooms in these Case 2 waters than currently operational MODIS algorithms. Our measured b_b/b and S_{nap} values indicated a dominant role by highly refractive non-algal particles in regulating backscattering variability in these waters, which was consistent with the strong correlation found between a_{nap} and particulate b_b. Relating these results to ocean color data, we found that b_b is the main factor driving observed variability in $R_{rs}(670)$, a quantity that can be measured remotely. Retrieval of particulate b_b from satellite measured $R_{rs}(670)$ can be applied to remotely monitor distribution and concentrations of highly refractive suspended particles in this region of the Bay. Moreover, retrieval of non-algal particulate absorption from the reflectance signal at 670 nm could be used in conjunction with inversion of UV-blue wavelengths to derive CDOM absorption in these Case 2 waters. Separating contribution by these two similarly absorbing, but non-covarying, components to total light absorption is particularly useful for remote sensing of CDOM and studies on dissolved organic carbon cycling in coastal waters. Quantitative analysis of particulate composition and measurements of the differences in the optical characteristics (i.e. S_{nap} and b_b) between organic detrital and inorganic

mineral suspended particles are needed to improve interpretation of remote sensing in coastal regions like Chesapeake Bay where non-algal particles often dominate the backscattered signal.

Acknowledgements

Funds for this work were provided by NASA-Goddard Space Flight Center, the University of Maryland, and the Smithsonian Pre-doctoral Fellowship program. Field work on Chesapeake Bay was funded in part by the Coastal Intensive Site Network (CISNet) program of the United States Environmental Protection Agency through grant R826943-01-0. We thank K. Yee, D. Sparks, M. Mallonee and S. Benson for assistance in the field and laboratory.

References

Aas, E., 1981. The refractive index of phytoplankton. Rep. 46. Institute of Geophysics, University of Oslo, Oslo, Norway, 61 pp.

Aas, E., 1996. Refractive index of phytoplankton derived from its metabolite composition. Journal of Plankton Research 18, 2223–2249.

Austin, R.W., 1974. The remote sensing of spectral radiance from below the ocean surface. In: Jerlov, N.G., Steemann-Nielsen, E. (Eds.), Optical Aspects of Oceanography. Academic Press, London, New York, pp. 317–344.

Babin, M., Stramski, D., Ferrari, G., Clauster, H., Bricaud, A., Obelensky, G., Hoepffner, N., 2003. Variations in the light absorption coefficients of phytoplankton, nonalgal particles, and dissolved organic matter in coastal waters around Europe. Journal of Geophysical Research 108 (C7), 3211.

Binding, C.E., Bowers, D.G., Mitchelson-Jacob, E.G., 2003. An algorithm for the retrieval of suspended sediment concentrations in the Irish Sea from SeaWiFS ocean colour satellite imagery. International Journal of Remote Sensing 24 (19), 3791–3806.

Blough, N.V., Del Vecchio, R., 2002. Chromophoric dissolved organic matter (CDOM) in the coastal environment. In: Hansell, D.A., Carlson, C.A. (Eds.), Biogeochemistry of Marine Dissolved Organic Matter. Academic Press, pp. 509–546.

Boss, E., Pegau, W.S., Lee, M., Twardowski, M.S., Shybanov, E., Korotaev, G., Baratange, F., 2004. The particulate backscattering ratio at LEO 15 and its use to study particles composition and distribution. Journal of Geophysical Research 109 (C01014). doi:10.1029/2002JC001514.

Bowers, D.G., Harker, G.E.L., Stephan, B., 1996. Absorption spectra of inorganic particles in the Irish Sea and their relevance to remote sensing of chlorophyll. International Journal of Remote Sensing 17 (12), 2449–2460.

Bricaud, A., Babin, M., Morel, A., Claustre, H., 1995. Variability in the chlorophyll-specific absorption coefficients of natural phytoplankton: analysis and parameterization. Journal of Geophysical Research 100 (C7), 13321–13332.

Carder, K.L., Betzer, P.R., Eggimann, D.W., 1974. Physical, chemical, and optical measures of suspended particle concentrations: their intercomparison and application to the west African shelf. In: Gibbs, R.J. (Ed.), Suspended Solids in Water. Plenum, New York, pp. 173–193.

Carder, K.L., Chen, F.R., Cannizzaro, J.P., Campbell, J.W., Mitchell, B.G., 2004. Performance of the MODIS semi-analytical ocean color algorithm for chlorophyll-a. Advances in Space Research 33 (7), 1152–1159.

Carder, K.L., Chen, R.F., Cannizzaro, J.P., 2002. "Case 2 Chlorophyll a" MODIS Ocean Science Team Algorithm Theoretical Basis Document, ATBD 19, Version 6.

Carder, K.L., Hawes, S.K., Baker, K.A., Smith, R.C., Steward, R.G., Mitchell, B.G., 1991. Reflectance model for quantifying chlorophyll a in the presence of productivity degradation products. Journal of Geophysical Research 96, 20599–20611.

Clark, D.K., 1997. Bio-Optical Algorithms Case 1 Waters, MODIS Algorithm Theoretical Basis Document.

Dall'Olmo, G., Gitelson, A.A., Rundquist, D.C., Leavitt, B., Barrow, T., Holz, J.C., 2005. Assessing the potential of SeaWiFS and MODIS for estimating chlorophyll concentration in turbid productive waters using red and near-infrared bands. Remote Sensing of Environment 96 (2), 176–187.

Darecki, M., Stramski, D., 2004. An evaluation of MODIS and SeaWiFS bio-optical algorithms in the Baltic Sea. Remote Sensing of Environment 89 (3), 326–350.

Ferrari, G.M., Bo, F.G., Babin, M., 2003. Geo-chemical and optical characterizations of suspended matter in European coastal waters. Estuarine, Coastal and Shelf Science 57, 17–24.

Gallegos, C.L., Neale, P.J., 2002. Partitioning spectral absorption in case 2 waters: discrimination of dissolved and particulate components. Applied Optics 41, 4220–4233.

Garver, S.A., Siegel, D.A., 1997. Inherent optical property inversion of ocean color spectra and its biogeochemical interpretation. I. Time series from the Sargasso Sea. Journal of Geophysical Research 102, 18607–18625.

Glibert, P.M., Conley, D.J., Fisher, T.R., Harding, L.W., Malone, T.C., 1995. Dynamics of the 1990 winter/spring bloom in Chesapeake Bay. Marine Ecology Progress Series 122, 22–43.

Gons, H.J., 1999. Optical teledetection of chlorophyll a in turbid inland waters. Environmental Science & Technology 33, 1127–1133.

Gordon, H.R., Brown, O.B., Evans, R.H., Brown, J.W., Smith, R.C., Baker, K.S., Clark, D.K., 1988. A semi-analytic model of ocean color. Journal of Geophysical Research 93, 10909–10924.

Gordon, H.R., Ding, K., 1992. Self-shading of in-water optical instruments. Limnology and Oceanography 37, 491–500.

Gordon, H.R., Brown, O.B., Jacobs, M.M., 1975. Computed relationships between the inherent and apparent optical properties of a flat homogeneous ocean. Applied Optics 14, 417–427.

Gordon, H.R., Voss, K.J., 1999. MODIS Normalized Water-leaving Radiance, Algorithm Theoretical Basis Document, Version 4, MOD 18.

Gower, J.F.R., Lin, S., Borstad, G.A., 1984. The information content of different optical spectral ranges for remote chlorophyll estimation in coastal waters. International Journal of Remote Sensing 5, 349–364.

Green, R.E., Sosik, H.M., Olson, R.J., 2003. Contributions of phytoplankton and other particles to inherent optical properties in New England continental shelf waters. Limnology and Oceanography 48 (6), 2377–2391.

Gregg, W.W., Conkright, M.E., 2001. Global seasonal climatologies of ocean chlorophyll: blending in situ and satellite data for the CZCS era. Journal of Geophysical Research 106, 2499–2515.

Harding Jr., L.W., Magnuson, A., Mallonee, M.E., 2005. Bio-optical and remote sensing observations in Chesapeake Bay. Estuarine, Coastal and Shelf Science 62, 75–94.

Harding, L.W., Magnuson, A., 2002. Bio-optical and remote sensing observations in Chesapeake Bay. In: Fargion, G.S., McClain, C.R. (Eds.), SIMBIOS Project 2001 Annual Report. NASA/TM, pp. 52–62.

Harding, L.W., Itsweire, E.C., Esaias, W.E., 1992. Determination of phytoplankton chlorophyll concentrations in the Chesapeake Bay with aircraft remote sensing. Remote Sensing of Environment 40, 79–100.

Harding, L.W., Perry, E., 1997. Long-term increase of phytoplankton biomass in Chesapeake Bay, 1950–94. Marine Ecology Progress Series 157, 39–52.

Hoge, F.E., Swift, R.N., 1981. Application of the NASA Airborne Oceanographic Lidar to the mapping of chlorophyll and other organic pigments. In: Campbell, J.W., Thomas, J.P. (Eds.), Chesapeake Bay Plume Study – Superflux 1980. NASA Conf. Publ. 2188, 81. NOAA/NEMP III. ABCDFG 0042.

van de Hulst, H.C., 1981. Light Scattering by Small Particles. Dover, Mineola, NY, 470 pp.

Jeffrey, S.W., Humphrey, G.F., 1975. New spectrophotometric equations for determining chlorophyll a, b, c, and c2 in higher plants algae and natural phytoplankton. Biochemie and Physiologie der Pflanzen 167, 191–194.

Johnson, D.R., Weidemann, A., Arnone, R., Davis, C.O., 2001. Chesapeake Bay outflow plume and coastal upwelling events: physical and optical properties. Journal of Geophysical Research 106 (C6), 11613–11622.

Kemp, W.M., Boynton, W.B., 1992. Benthic-pelagic interactions: nutrient and oxygen dynamics. In: Smith, D.E., Leffler, M., Mackiernan, G. (Eds.),

Oxygen Dynamics in the Chesapeake Bay: A Synthesis of Research. Maryland Sea Grant College, College Park, MD, pp. 149–221.

Kirk, J.T.O., 1984. Dependence of relationship between inherent and apparent optical properties of water on solar altitude. Limnology and Oceanography 29, 350–356.

Kirk, J.T.O., 1992. Monte Carlo modeling of the performance of the reflective tube absorption meter. Applied Optics 31, 6463–6468.

Lee, Z.P., Carder, K.L., Hawes, S.H., Steward, R.G., Peacock, T.G., Davis, C.O., 1994. A model for interpretation of hyperspectral remote-sensing reflectance. Applied Optics 33, 5721–5732.

Lobitz, B., Johnson, L., Mountford, K., Stokely, P., 1998. AVIRIS analysis of water quality in the Chesapeake Bay. Proceedings of the Fifth International Conference on Remote Sensing for Marine and Coastal Environments, vol. 1. 5–7 October, San Diego CA.

Longhurst, A., Sathyendranath, S., Platt, T., Caverhill, C., 1995. An estimate of global primary production in the ocean from satellite radiometer data. Journal of Plankton Research 17, 1245–1271.

Maffione, R.A., Dana, D.R., 1997. Instruments and methods for measuring the backward-scattering coefficient of ocean waters. Applied Optics 36, 6057–6067.

Magnuson, A., Harding, L.W., Mallonee, M.E., Adolf, J.E., 2004. Bio-optical model for Chesapeake Bay and the middle Atlantic bight. Estuarine, Coastal and Shelf Science 61, 403–424.

Malone, T.C., 1992. Effects of water column processes on dissolved oxygen: nutrients, phytoplankton and zooplankton. In: Smith, D., Leer, M., Mackiernan, G. (Eds.), Oxygen Dynamics in Chesapeake Bay: A Synthesis of Research. University of Maryland Sea Grant, College Park, MD, pp. 61–112.

Maritorena, S., Siegel, D.A., Peterson, A.R., 2002. Optimization of a semianalytical ocean color model for global-scale applications. Applied Optics 41, 2705–2714.

McClain, C.R., Feldman, G.C., Hooker, S.B., 2004. An overview of the SeaWiFS project and strategies for producing a climate research quality global ocean bio-optical time series, Deep Sea Research. II. Topical Studies in Oceanography 51, 5–42.

Mitchell, G., Bricaud, A., Carder, K., Cleveland, J., Ferrari, G., Gould, R., Kahru, M., Kishino, M., Maske, H., Moisan, T., Moore, L., Nelson, N., Phinney, D., Reynolds, R., Sossik, H., Stramski, D., Tassan, S., Trees, C.C., Weidemann, A., Wieland, J., Vodacek, A., 2000. Determination of spectral absorption coefficients of particles, dissolved material and phytoplankton for discrete water samples. In: Fargion, G.S., Mueller, J.L. (Eds.), Ocean Optics Protocols for Satellite Ocean Color Sensor Validation, Revision 2. NASA/TM-2000-209966 (Chapter 12).

Mobley, C.D., 1994. Light and Water: Radiative Transfer in Natural Waters. Academic Press, San Diego, CA.

Mobley, C.D., Sundman, L.K., Boss, E., 2002. Phase function effects on oceanic light fields. Applied Optics 41, 1035–1050.

Mobley, C.D., Gentili, B., Gordon, H.R., Jin, Z., Kattawar, G.W., Morel, A., Reinersman, P., Stamnes, K., Stavn, R., 1993. Comparison of numerical models for the computation of underwater light fields. Applied Optics 32 (36), 7484–7504. See also http://www.hydrolight.info.

Montagnes, D.J., Berges, J.A., Harrison, P.J., Taylor, F.J.R., 1994. Estimation of carbon, nitrogen, protein, and chlorophyll a from volume in marine phytoplankton. Limnology and Oceanography 39, 1044–1060.

Moore, C., Twardowski, M.S., Zaneveld, J.R.V., 2000. The ECO VSF – a multi-angle scattering sensor for determination of the volume scattering function in the backward direction. Proceedings from Ocean Optics XV, 16–20 October, Monaco.

Morel, A., 1974. Optical properties of pure water and pure seawater. In: Jerlov, N.G., Steeman, E. (Eds.), Optical Aspects of Oceanography. Academic, London, pp. 1–24.

Morel, A., Gentili, B., 1991. Diffuse reflectance of oceanic waters: its dependence on sun angle as influenced by the molecular scattering contribution. Applied Optics 30, 4427–4438.

Morel, A., Gentili, B., 1993. Diffuse reflectance of oceanic waters. II. Bidirectional aspects. Applied Optics 32, 6864–6879.

Morel, A., Mueller, J.L., 2002. Normalized water-leaving radiance and remote sensing reflectance: bidirectional reflectance and other factors. In: Mueller, J.L., Fargion, G.S. (Eds.), Ocean Optics Protocols for Satellite Ocean Color Sensor Validation, Rev3, vol 2. NASA/TM-2002-210004. (Chapter 13), pp. 183–210.

Morel, A., Prieur, L., 1977. Analysis of variations in ocean color. Limnology and Oceanography 22, 709–722.

Morel, A., Antoine, D., Gentili, B., 2002. Bidirectional reflectance of oceanic waters: accounting for Raman emission and varying particle scattering phase function. Applied Optics 41 (30), 6289–6306.

O'Reilly, J.E., Maritorena, S., Siegel, D., O'Brien, M.C., Toole, D., Mitchell, B.G., Kahru, M., Chavez, F.P., Strutton, P., Cota, G., Hooker, S.B., McClain, C.R., Carder, K.L., Muller-Karger, F., Harding, L., Magnuson, A., Phinney, D., Moore, G.F., Aiken, J., Arrigo, K.R., Letelier, R., Culver, M., 2000. Ocean color chlorophyll a algorithms for SeaWiFS, OC2, and OC4: Version 4. In: Hooker, S.B., Firestone, E.R. (Eds.), SeaWiFS Postlaunch Technical Report Series. SeaWiFS Postlaunch Calibration and Validation Analyses, Part 3, vol. 11. NASA, Goddard Space Flight Center, Greenbelt, MD, pp. 9–23.

Pegau, W.S., Gray, D., Zaneveld, J.R.V., 1997. Absorption and attenuation of visible and near-infrared light in water: dependence on temperature and salinity. Applied Optics 36, 6035–6046.

Pope, R.M., Fry, E.S., 1997. Absorption spectrum (380–700 nm) of pure water. II. Integrating measurements. Applied Optics 36, 8710–8723.

Preisendorfer, R.W., 1976. Hydrological Optics (6 volumes). US Department of Commerce, NOAA, Honolulu, HA.

Ruddick, K.G., Gons, H.J., Rijkeboer, M., Tilstone, G., 2001. Optical remote sensing of chlorophyll a in case 2 waters by use of an adaptive two-band algorithm with optimal error properties. Applied Optics 40 (21), 3575–3585.

Satlantic, 2002. Operation Manual for the MicroPro, Revision D, June 2002.

Smith, R.C., Baker, K.S., 1981. Optical properties of the clearest natural waters (200–800 nm). Applied Optics 20, 177–184.

Stramski, D., 1999. Refractive index of planktonic cells as a measure of cellular carbon and chlorophyll a content. Deep-Sea Research Part I 46, 335–351.

Stramski, D., Boss, E., Bogucki, D., Voss, K.J., 2004. The role of seawater constituents in light backscattering in the ocean. Progress in Oceanography 61 (1), 27–55.

Stramski, D., Morel, A., Bricaud, A., 1988. Modeling the light attenuation and scattering by spherical phytoplankton cells: a retrieval of the bulk refractive index. Applied Optics 27, 3954–3956.

Stramski, D., Reynolds, R.A., Kahru, M., Mitchell, B.G., 1999. Estimation of particulate organic carbon in the ocean from satellite remote sensing. Science 285 (5433), 239–242.

Sullivan, J.M., Twardowski, M.S., Donaghay, P.L., Freeman, S., 2002. Particulate bulk refractive index distributions in coastal regions as determined from backscattering ratio measurements. Proceedings from Ocean Optics XVI, 18–22 November, Santa Fe.

Sydor, M., Arnone, R.A., 1997. Effect of suspended particulate and dissolved organic matter on remote sensing of coastal and riverine waters. Applied Optics 36, 6905–6912.

Twardowski, M., Boss, E., Macdonald, J.B., Pegau, W.S., Barnard, A.H., Zaneveld, J.R.V., 2001. A model for estimating bulk refractive index from the optical backscattering ratio and the implications for understanding particle composition in case I and case II waters. Journal of Geophysical Research 106, 14129–14142.

Tzortziou, M., 2004. Measurements and characterization of optical properties in the Chesapeake Bay's estuarine waters, using in-situ measurements, MODIS satellite observations and radiative transfer modelling. PhD Dissertation, Department of Meteorology, University of Maryland, College Park, MD.

Tzortziou, M., Herman, J., Gallegos, C., Neale, P., Subramaniam, A., Harding, L., Ahmad, Z., 2006. Bio-optics of the Chesapeake Bay from measurements and radiative transfer closure. Estuarine, Coastal and Shelf Science 68, 348–362.

Verity, P.G., Robertson, C.Y., Tronzo, C.R., Andrews, M.G., Nelson, J.R., Sieracki, M.E., 1992. Relationships between cell volume and the carbon and nitrogen content of marine photosynthetic nanoplankton. Limnology and Oceanography 37, 1434–1446.

Voipo, A., 1981. The Baltic Sea. Elsevier Science, New York, 416 pp.

Voss, K.J., 1989. Use of the radiance distribution to measure the optical absorption coefficient in the ocean. Limnology and Oceanography 34, 1614–1622.

Voss, K.J., Morel, A., 2005. Bidirectional reflectance function for oceanic waters with varying chlorophyll concentrations: measurements versus predictions. Limnology and Oceanography 50 (2), 698–705.

Wozniak, S.B., Stramski, D., 2004. Modeling the optical properties of mineral particles suspended in seawater and their influence on ocean reflectance and chlorophyll estimation from remote sensing algorithms. Applied Optics 43 (17), 3489–3503.

Yentsch, C.S., 1993. CZCS: its role in the study of the growth of oceanic phytoplankton. In: Barale, V., Schlittenhardt, P.M. (Eds.), Ocean Colour: Theory and Applications in a Decade of CZCS Experience. Kluwer Academic Publishers, Dordrecht, The Netherlands, pp. 17–32.

Yoder, J.A., Kennelly, M.A., 2003. Seasonal and ENSO variability in global ocean phytoplankton chlorophyll derived from 4 years of SeaWiFS measurements. Global Biogeochemical Cycles 17 (4).

Zibordi, G., Ferrari, G.M., 1995. Instrument self-shading in underwater optical measurements: experimental data. Applied Optics 34, 2750–2754.